

Extracellular Matrix Protein Coating of Processed Fish Scales Improves Human Corneal Endothelial Cell Adhesion and Proliferation

Yi-Jen Hsueh^{1,2,*}, David Hui-Kang Ma^{1-3,*}, Kathleen Sheng-Chuan Ma¹, Tze-Kai Wang^{1,2}, Cheng-Hung Chou⁴, Chien-Cheng Lin⁴, Min-Chang Huang⁴, Li-Jyuan Luo⁵, Jui-Yang Lai^{2,6,7}, and Hung-Chi Chen^{1,2,8}

¹ Limbal Stem Cell Laboratory, Department of Ophthalmology, Chang Gung Memorial Hospital, Linkou, Taiwan

² Center for Tissue Engineering, Chang Gung Memorial Hospital, Linkou, Taiwan

³ Department of Chinese Medicine, College of Medicine, Chang Gung University, Taoyuan, Taiwan

⁴ Department of Research, Body Organ Biomedical Corporation, Taipei, Taiwan

⁵ Department of Chemical and Materials Engineering, Chang Gung University, Taoyuan, Taiwan

⁶ Institute of Biochemical and Biomedical Engineering, Chang Gung University, Taoyuan, Taiwan

⁷ Department of Materials Engineering, Ming Chi University of Technology, New Taipei City, Taiwan

⁸ Department of Medicine, College of Medicine, Chang Gung University, Taoyuan, Taiwan

Correspondence: Hung-Chi Chen, Limbal Stem Cell Laboratory, Department of Ophthalmology, Chang Gung Memorial Hospital, no. 5, Fushing Street, Kweishan District, Taoyuan City 33305, Taiwan. e-mail: mr3756@cgmh.org.tw

Jui-Yang Lai, Institute of Biochemical and Biomedical Engineering, Chang Gung University, no. 259 Wen-Hwa 1st Road, Kweishan District, Taoyuan City, 33305, Taiwan. e-mail: jyilai@mail.cgu.edu.tw

Received: 24 September 2018

Accepted: 19 March 2019

Published: 30 May 2019

Keywords: human corneal endothelial cells; fish scales; extracellular matrix protein; surface coating; cytocompatibility

Citation: Hsueh Y-J, Ma DH-K, Ma KS-C, Wang T-K, Chou C-H, Lin C-C, Huang M-C, Luo L-J, Lai J-Y, Chen H-C. Extracellular matrix protein coating of processed fish scales improves human corneal endothelial cell adhesion and proliferation. *Trans Vis Sci Tech.* 2019;8(3):27, <https://doi.org/10.1167/tvst.8.3.27>
Copyright 2019 The Authors

Purpose: Corneal transplantation can treat corneal endothelial diseases. Implanting cultivated human corneal endothelial cells (HCECs) via a cell carrier has clinical value as an alternative therapeutic strategy. This study was performed to compare the feasibility of fish scales and other biomaterials (gelatin and chitosan) as cell carriers and to investigate the effects of an extracellular matrix (ECM) protein coating to improve the cytocompatibility of fish scales.

Methods: The physical properties of gelatin, chitosan, and fish scales were compared. Immortalized HCECs (B4G12) were cultured on processed fish scales, which were coated with fibronectin, laminin, collagen IV, or FNC Coating Mix. Cell attachment and proliferation were evaluated by immunofluorescence, cell counting, and bromodeoxyuridine (BrdU) labeling assays. Immunoblots were used to examine the expression levels of integrin-linked kinase (ILK), phosphate-ILK, β -catenin, p63, and cell cycle mediators (cyclin D1 and p27^{Kip1}).

Results: The transparency of processed fish scales was better than that of chitosan, while the strength was higher than that of gelatin. The laminin, collagen IV, and FNC coatings facilitated B4G12 cell adhesion and proliferation, while fibronectin only facilitated cell adhesion. The laminin, collagen IV, and FNC coatings also upregulated phosphate-ILK and p63 expression. In addition, the FNC coating activated cell cycle mediators.

Conclusion: ECM protein-coated processed fish scales can serve as a novel cell carrier to facilitate the development of HCEC transplantation.

Translational Relevance: Improving the physical properties and cytocompatibility of fish scales as a cell carrier will facilitate the transplantation of HCECs into corneas for the purpose of cell therapy.

Introduction

The inner surface of the cornea is comprised of a single layer of corneal endothelium, formed by human corneal endothelial cells (HCECs). The major function of the corneal endothelium is to maintain a constant water content in the corneal stroma. HCECs rely on the intercell barrier formed by the tight junction protein zona occlusion-1 (ZO-1)^{1,2} and the water pump protein Na/K-ATPase (ATPase)³⁻⁵ to prevent corneal edema and to maintain corneal transparency; therefore, these proteins are often used as markers when characterizing the morphology and function of HCECs. The human corneal endothelium density is approximately 3500 to 4000 cells/mm² at birth, which gradually decreases and stabilizes at 2000 to 3000 cells/mm² with age.⁶⁻⁸ When the HCEC density drops below 1000 cells/mm², as can be observed in diseases such as Fuch's endothelial corneal dystrophy, cataract surgery-caused damage, corneal hypoxia, and glaucoma, the corneal endothelium loses its water-regulating function. Once the corneal endothelium loses its function and corneal edema occurs, penetrating keratoplasty is usually required to restore vision.

Over the past decade, lamellar corneal transplantation, in which only the damaged part of the cornea is replaced, rather than the entire cornea, has been increasingly used in place of penetrating keratoplasty for corneal transplantation. This procedure not only preserves the mechanical strength of the cornea but also reduces the occurrence of transplantation rejection. According to the American Eye Bank Association, nearly half of corneal transplant cases in the United States are associated with endothelial keratoplasty. Likewise, over 50% of corneal transplantation cases in Taiwan are due to endothelial cell dysfunction.⁹ Therefore, endothelial keratoplasty has become an increasingly popular option for corneal transplantation.

The Descemet stripping automated endothelial keratoplasty (DSAEK) procedure is one of the major types of endothelial keratoplasty,¹⁰ which has the advantages of reduced postoperative refraction changes, faster wound healing, the ability to maintain the corneal surface integrity, and increased resistance to external blows. However, for DSAEK, donor corneas are still required. In 2009, Honda et al.¹¹ used endothelium-removed human corneal lamella as a carrier to transplant cultivated HCECs with the DSAEK technique, which successfully cleared the

swollen corneas of rabbits. Transplanting cultivated HCECs into the eye using the DSAEK technique is called culture-based DSAEK (c-DSAEK). The development of c-DSAEK is important because of the long-standing corneal shortage in Asia and the universal issue that most donated corneas are aged corneas, with reduced endothelial densities.

Regarding the development of HCEC carriers, Doillon et al.¹² first used collagen as a carrier material in 2003. The use of various biomedical materials, including cross-linked hyaluronic acid,¹³ collagen/chitosan/sodium hyaluronate,¹⁴ chitosan/polycaprolactone blends,¹⁵ and heparin-modified gelatin,¹⁶ has also been reported. However, the mechanical strength and cytocompatibility of the abovementioned materials must be improved. Because the structural properties and strengths of synthesized biomedical materials are usually inferior to those of animal corneas, another source of carrier material is decellularized animal corneas.¹⁷ However, the supply of animal corneas is also limited, and animal corneas can be difficult to obtain due to the high costs of quarantine and the screening of zoonoses.

Like corneas, tilapia fish scales are a biomaterial with the potential for use as a natural, collagen-based cell carrier that can be obtained in large quantities.¹⁸ Tilapia fish scales are primarily composed of type I collagen and hydroxyapatite.¹⁹ After decalcification, the collagen fibers in tilapia scales are arranged in neat layers, with collagen fibers that are arranged perpendicularly to those in adjacent layers, similar to the arrangement of corneal stroma layers.²⁰⁻²² Therefore, fish scales show excellent light transmission after decalcification. Due to properties such as biodegradability and low rejection, fish scales have been used to make bone nails and during fracture fixation to speed up the healing process.²³ Fish scales have also been tested as artificial corneal implants because of their excellent light transmission.²⁴ This material also exhibits good biosafety after decellularization.²⁴⁻²⁶

Suitability for cell attachment and growth is another important characteristic of a cell carrier. Cells bind to extracellular matrix (ECM) proteins through hemidesmosomes (formed by the transmembrane protein integrin). Therefore, ECM protein coating of a surface can effectively improve the carrier's cytocompatibility.²⁷ Recent studies have revealed that integrin signaling is also involved in regulating cell proliferation.^{28,29} The integrin pathway may affect the cell cycle via phosphatidylinositol 3-kinase (PI3K) signaling.³⁰ This pathway also affects cyclin D1, via the integrin-linked kinase/Protein

Kinase B (ILK/Akt) pathway^{31,32} or the inhibition of p27^{Kip1}, which regulates cell proliferation.^{33,34} The transcription factor p63 is reportedly involved in the regulation of corneal epithelial cell proliferation,³⁵ and previously, we have observed that surface changes for the carrier may affect cell proliferation through the ILK/ β -catenin/p63 signaling cascade.³⁶ It has been reported that integrins participate in the proliferation control of HCECs,³⁷ and we have observed that PI3K/Akt signaling is involved in cyclin D1 and p27^{Kip1} expression and cell proliferation in B4G12 cells.³⁸ Therefore, the ECM protein coating of fish scales may affect cell proliferation through the abovementioned pathways.

Recently, Parekh et al.²⁷ reported the use of tilapia fish scales as an HCEC carrier and found that fish scales required surface coating with an FNC Coating Mix to facilitate cell adhesion. In this study, we further compared tilapia fish scales with other reported HCEC carrier materials (gelatin and chitosan) and found that processed fish scales have several advantages as a cell carrier, including transparency, strength, and biodegradability. We also confirmed that ECM protein-coated and processed fish scales have excellent cytocompatibility and that ECM protein coating can promote cell proliferation. The results of this study show that ECM protein-coated fish scales can be used as a novel HCEC carrier that will benefit cell therapies.

Materials and Methods

Fetal bovine serum (FBS), phosphate-buffered saline (PBS), trypsin-ethylenediaminetetraacetic acid (EDTA), gentamicin, amphotericin B, and an Alexa-Fluor-conjugated secondary immunoglobulin (Ig) G antibody were purchased from Invitrogen (Carlsbad, CA). Dimethyl sulfoxide (DMSO), RPMI 1640 vitamin solution, Hoechst 33342 dye, methanol, and Triton X-100 were purchased from Sigma-Aldrich (St. Louis, MO). Recombinant human basic fibroblast growth factor (FGF) was purchased from Peprotech (London, UK). Collagenase A was purchased from Roche Applied Science (Indianapolis, IN).

A rabbit polyclonal p27^{Kip1} (C-19) antibody was purchased from Santa Cruz Biotechnology (Santa Cruz, CA). Mouse β -catenin (clone 15B8) and cyclin D1 (clone CD1.1) antibodies and a rabbit polyclonal lamin B1 (ab16048) antibody were purchased from Abcam (La Jolla, CA). A mouse bromodeoxyuridine (BrdU; RPN20Ab) antibody was purchased from GE Healthcare Amersham (Chalfont St. Giles, UK). A

mouse ZO-1 (clone ZO1-1A12) antibody was purchased from Invitrogen. Mouse Na/K-ATPase (clone C464.6), GAPDH (clone 6C5), and p63 (clone 4A4) antibodies were purchased from Millipore (Billerica, MA). A rabbit polyclonal ILK (3862) antibody was purchased from Cell Signaling Technologies (Beverly, MA). A rabbit polyclonal phospho-ILK (T173) antibody (AP7651f) was purchased from Abgent (San Diego, CA). All plastic cell culture ware was obtained from Corning Incorporated Life Sciences (Acton, MA).

The tilapia fish scales were obtained from and prepared by Body Organ Biomedical Corporation (Taiwan). Briefly, fish scales were harvested from whole fish skin and were immediately washed using distilled water (unprocessed). The fish scales were treated with a decellularization (half-processed) and decalcification (processed) process, as described in a previous study.³⁹ The processed fish scales (13 mm [diameter], 0.30–0.35 mm [thickness]) were then stored in PBS and sterilized by gamma-irradiation for further studies.

Physical Property Tests

Optical Transmittance Measurements

All carrier material samples were immersed in deionized water and then blotted with tissue paper to remove excess water from the surface. The gross appearance of the swollen materials was photographed with a digital camera (Nikon, Melville, NY). Optical transmittance was measured using a UV-visible spectrophotometer (Thermo Fisher Scientific, Waltham, MA), as previously described.^{24,40} In brief, the test specimen was placed in a cell in the middle of the sample holder. During the spectrometry measurements of carriers that operate in the spectral range of 400 to 700 nm, the reference sample consisted of only the material holder, and the test sample consisted of the holder with the carrier in place.

Mechanical Strength Measurements

Uniaxial tensile tests were performed according to our previously published procedures.⁴¹ Dumbbell-shaped specimens were fabricated by cutting carrier sheets with a suitable mold under pressure. The gauge length of the specimens was 20 mm, and the width was 5 mm. Sample thickness was measured with a Pocket Leptoskop electronic thickness gauge (Karl Deutsch, Germany). The mechanical properties of all samples were measured at 25°C, with 50% relative humidity, using an Instron Mini 44 universal testing

machine (Canton, MA). The results were averaged over three independent runs.

Degradation Studies

The extent of degradation was measured according to our previously published procedures.⁴² Each type of carrier material was first dried to constant weight (W_i) in vacuo and immersed in 1 mL of a balanced salt solution (BSS; pH 7.4) containing 12 μg of collagenase (Col I from *Clostridium histolyticum*, EC 3.4.24.3) at 34°C, with reciprocal shaking in a thermostatically controlled water bath. The degradation medium was replaced regularly with fresh buffer containing the same concentration of enzyme. At specific time intervals, the degraded samples were further dried in vacuo and weighed to determine the dry weight (W_d). The percentage weight loss (%) was calculated as $((W_i - W_d)/W_i) \times 100$. The results were averaged over three independent measurements.

Fish Scale Surface Coating With ECM Proteins

The processed fish scales were treated with antibiotics and washed with PBS to remove residual antibiotics. The samples were placed in ECM protein solutions, including fibronectin (5 $\mu\text{g}/\text{cm}^2$, Sigma-Aldrich), laminin (2 $\mu\text{g}/\text{cm}^2$, Sigma-Aldrich, cat# L6274, from human placenta), collagen IV (10 $\mu\text{g}/\text{cm}^2$, Corning, Acton, MA), and FNC Coating Mix (Athena Environmental Sciences, Inc., Baltimore, MD; ingredients include albumin, collagen I and fibronectin), for half an hour. Afterwards, the samples were removed, air-dried, and placed in human endothelial serum-free medium (HESFM).

Cell Preparation

This study adhered to the tenets of the Declaration of Helsinki and was approved by the Institutional Review Board of Chang Gung Memorial Hospital (institutional review board approval number 201600515B0). Immortalized HCECs (B4G12 cells) were purchased from Creative Bioarray (Shirley, NY). The cells were cultured in HESFM (Invitrogen) supplemented with 2% FBS and 10 ng/mL basic FGF. The isolation and culture of primary HCECs were performed as described previously.⁴³ Briefly, after removing the central region for clinical transplantation, the human donor corneas ($n = 2$; OS/OD, aged 61 years) were rinsed with wash medium (containing Opti-MEM, 200 $\mu\text{g}/\text{mL}$ gentamicin and 10 $\mu\text{g}/\text{mL}$ amphotericin B), and the corneal endothelium was

stripped. Following digestion at 37°C for 24 hours with 0.5 mg/mL collagenase A in the wash medium, the stripped corneal endothelium formed cell aggregates. The cell aggregates were cultured in two wells of eight-well Lab-Tek II chamber slides (Nalge Nunc International, Rochester, NY), coated with FNC Coating Mix (Athena Environmental Sciences) in HCEC growth medium (containing Opti-MEM, 10% FBS, 20 ng/mL human epidermal growth factor (EGF), 10 ng/mL basic FGF, RPMI 1640 vitamin solution, 25 $\mu\text{g}/\text{mL}$ gentamicin, and 1.25 $\mu\text{g}/\text{mL}$ amphotericin B). After 3 weeks, the HCEC aggregates had expanded into a cell monolayer, and the cells were subcultured on FNC-coated processed fish scales (13 mm diameter).

Cell Adhesion Test

Fish scales were placed in a 24-well culture plate, and B4G12 cells (2.5×10^5 cells/well) were then subcultured on the surfaces of the fish scales. After the cells attached to the surfaces of the fish scales, the scales were transferred to another 24-well plastic culture plate. Cell attachment was checked 48 hours later, using phase contrast microscopy, or the cells were separated 24 hours later for cell counting.

Cell Counting

The cells from the different groups were treated with 0.5 mL trypsin, and then 100 μL cell suspension was mixed with 100 μL trypan blue. Then, 20 μL of this mixture was loaded onto a hemocytometer, covered with a coverslip, and examined on an inverted microscope at 100 \times magnification. The cell numbers in four squares were counted, averaged, and then multiplied by the dilution factor to obtain the number of cells per milliliter in the cell suspension. The counting process was repeated three times for each group.

Cell Proliferation Test

Cell proliferation was evaluated by cell counting and with a BrdU labeling assay. For cell counting, the cells were seeded onto the surface of the fish scales, and the culture medium was changed to serum-free medium on the following day. On days 1 to 4, cells were counted using a hemocytometer, as described above. For the BrdU labeling assay, cells from the different treatment groups were labeled with BrdU for 2.5 hours (Cell Proliferation Kit, GE Healthcare Amersham), followed by washing with cold PBS to remove the culture medium. The cells were fixed with

100% cold methanol for 10 minutes, and 5% BSA was added for 30 minutes to block nonspecific binding. Then, an anti-BrdU monoclonal antibody was mixed with DNase I and added to the sample at room temperature for 1 hour. A secondary antibody (1:100, Chemicon, Temecula, CA) was then added at room temperature for 30 minutes, followed by Hoechst 33342 staining and mounting. The samples were then examined using an IF conjugation microscope (TCS SP2-MP system, Leica).

Scanning Electron Microscopy (SEM)

The samples were observed via SEM. First, the sample was washed three times with PBS (pH 7.5) and then fixed in 2% glutaraldehyde-PBS for 2 hours. The supernatant was then removed, the sample was washed three times with PBS, and fixed in OSO4-PBS for 2 hours. The supernatant was then removed, and the sample was washed with deionized water four times, followed by dehydration using an alcohol gradient and substitution in isoamyl acetate solution twice, for 20 minutes each. The sample was then dried in a CO₂ critical point dryer (LADD, Williston, VT). The dried sample was then placed on a holder, plated with platinum in a plating machine (SC502, Bio-Rad, Hercules, CA) and observed via SEM (ABT-32, JP).

Immunofluorescence

The cells were fixed in 4% formaldehyde for 15 minutes and washed with cold PBS to remove the fixative. After treatment with 0.2% Triton X-100 for 15 minutes, 5% bovine serum albumin was added to block nonspecific binding for 30 minutes, and primary antibody was added and incubated at room temperature for 1 hour. Secondary antibody was then added at room temperature for 30 minutes, followed by nuclear staining and mounting. Finally, the samples were examined under an immunofluorescence microscope (TCS SP2-MP system, Leica).

Protein Extraction

Nuclear Protein Extraction

Nuclear protein was extracted using a nuclear extraction kit (Affymetrix, Santa Clara, CA), according to the manufacturer's instructions. Briefly, cells were washed with precooled PBS to remove the culture medium, after which, 1× Buffer A (containing 1 mM dithiothreitol, 1× protease inhibitor, and 1× phosphatase inhibitor) was added, and the cells were incubated on ice for 15 minutes. The cells were then scraped off and centrifuged at 14,000 × g for 4

minutes at 4°C. The supernatant was discarded, and the pellet contained the nuclei. Then, 1× Buffer B (containing 1 mM DTT, 1× protease inhibitor, and 1× phosphatase inhibitor) was added, and the sample was vortexed for 10 seconds. The centrifuge tube was placed on ice for 1 hour, during which the sample was vortexed once every 20 minutes. Afterwards, the sample was centrifuged at 4°C at 14,000 × g for 5 minutes. The supernatant contained the nuclear proteins.

Total Protein Extraction

Cells were washed with precooled 1× PBS and then placed in Tissue Protein Extraction Reagent (T-PER, Pierce, Rockford, IL), supplemented with 1× protease inhibitor and 1× phosphatase inhibitor, for 10 minutes. The cells were scraped from the culture dish using a scraper, transferred into a centrifuge tube, placed on ice and ultrasound vibrated five times for 6 seconds each. The sample was centrifuged at 4°C for 15 minutes, and the resulting supernatant contained the total cell proteins.

Immunoblotting

The protein samples were quantified with Coomassie brilliant blue. Protein samples (10 µg) were taken from each group and separated via 10% sodium dodecyl sulfate-polyacrylamide gel electrophoresis (SDS-PAGE). The proteins were then transferred to polyvinylidene fluoride (PVDF). After 1 hour of blocking in 5% nonfat milk, the sample was incubated overnight with primary antibody at 4°C and then washed three times with phosphate buffered saline with tween 20 (PBST). After incubating with secondary antibody, anti-IgG-horseradish peroxidase (HRP), at room temperature for 1 hour, the blot was washed three times and developed using ECL Western Blotting Detection Reagents and an Analysis System Kit (GE Healthcare Amersham).

Quantitative Polymerase Chain Reaction (PCR)

RNA Extraction

The samples were washed with PBS, precooled on ice, and then mixed with a 10-fold volume of TRIzol reagent. The B4G12 cells on the surfaces of the scales were scraped off with a surgical blade and mixed well with chloroform (200 µL for each milliliter). After centrifugation, the aqueous layer was mixed with an equal volume of isopropanol and 20 µg of glycogen. The sample was incubated for 30 minutes at -80°C,

washed with 75% alcohol, and then resuspended in diethyl pyrocarbonate (DEPC).

Quantitative PCR (q-PCR) Analysis

q-PCR was performed using the TOOLS 2× SYBR q-PCR Mix (BIOTOOLS Co., Ltd., Taiwan). All reactions were performed on an ABI StepOne 7500 Fast Real-Time PCR System (Applied Biosystems, Waltham, MA). The primers used were as follows: ZO-1 forward, 5'-CAACATACAGTGACGCTTCACA-3'; ZO-1 reverse, 5'-CACTATTGACGTTTCCCCACTC-3'; ATPase (ATP1A1) forward, 5'-CTGTGGATTG-GAGCGATTCTT-3'; and ATPase reverse, 5'-TTA-CAACGGCTGATAGCACCA-3'. The process started with 40 amplification cycles, followed by a melt-curve analysis at 60°C for 1 minute. Finally, the amplification curve and the ΔC_t values were analyzed using Step One v2.0 software (Applied Biosystems). Glyceraldehyde 3-phosphate dehydrogenase (GAPDH) expression was used as a control for each gene. Each gene was analyzed in triplicate, and the mean values and standard deviations were calculated after dividing the ΔC_t values by the ΔC_t value of GAPDH.

Statistics

All tests were repeated three times, and the data are expressed as the mean \pm standard deviation. The data were analyzed with Microsoft Excel version 2010 (Redmond, WA), using a one-way analysis of variance, and $P < 0.05^*$ and $P < 0.01^{**}$ indicated significant differences between groups.

Results

Observations and Comparisons of the Physical Properties of the Cell Carrier Materials

Both gelatin and chitosan have previously been used as carriers for HCECs.^{12,14–16} Therefore, we first examined their physical properties to determine whether fish scales were superior to existing materials. The optical transmission values of the different carrier materials (including gelatin, chitosan, unprocessed fish scales, half-processed fish scales, and processed fish scales) were measured, as shown in the corresponding curved graphs (Fig. 1A). After processing, the optical transmission value of the fish scales increased 88%. The optical transmission value of the processed fish scales was higher than that of chitosan (43%) and lower than that of gelatin (97%). In Figure 1B, the results show that the mechanical strength of

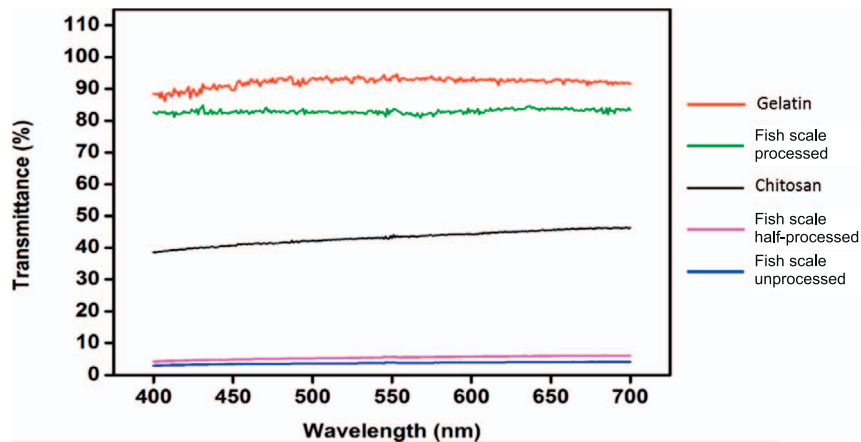
the fish scales decreased to 33 MPa after processing, which was higher than that of gelatin (7 MPa) and lower than that of chitosan (68 MPa). In addition, the results of the collagenase degradation test showed that gelatin was only detectable in the collagenase solution for less than 1 day, while chitosan, unprocessed fish scales, and half-processed fish scales were not degraded in the collagenase solution until day 14. The weight of the processed fish scales decreased in the collagenase solution over time, with losses of 50% on day 6 and 86% on day 14 (Fig. 2).

Fish Scale Cytocompatibility and Effects of ECM Protein Coating

B4G12 cells are a SV40-immortalized subclonal cell line, derived from primary HCECs that retain a normal morphology.⁴⁴ Given the scarce availability of cornea donors and the differences in HCECs among individual donors, B4G12 cells could be considered to be a cell source with higher homogeneity. B4G12 cells are able to expand and proliferate on noncoated plastic dishes (Supplementary Fig. S1A). However, when B4G12 cells were subcultured on the surfaces of noncoated fish scales, the cells failed to expand and instead agglomerated on the surfaces of the fish scales (Supplementary Figs. S1A, 3A). This phenomenon persisted after 3 weeks of culture. The aggregation of individual cells into clumps could be observed via SEM (Fig. 3B). The fish scale surface was then coated with ECM proteins, such as fibronectin (FN), laminin (LN), collagen IV (Col IV), and FNC coating mix (FNC), and B4G12 cells were subcultured on the surfaces of the coated fish scales. The cells successfully attached to and expanded on the surfaces of the coated fish scales (Fig. 3C). Specifically, the cells cultured on LN- and FNC-coated fish scales had greater densities (LN 467.1 ± 30.1 cells/mm², FNC 464.6 ± 26.5 cells/mm²) and showed polygonal morphologies. In contrast, the cells cultured on FN- and Col IV-coated fish scales had lower densities (FN 286.2 ± 15.1 cells/mm², Col IV 359.1 ± 18.9 cells/mm²) and showed irregular morphologies. Further, the cytocompatibility of FNC-coated fish scales with primary HCECs was also observed, and the results showed normal adhesiveness and polygonal morphology for primary HCECs on FNC-coated fish scales (Figs. 3D, 3E).

Because ZO-1 and ATPase expression have been used as HCEC markers, and their localization is essential for their functions, the expression levels and localization of ZO-1 and ATPase were examined using q-PCR, immunoblotting, and immunofluorescence.

(A).



(B).

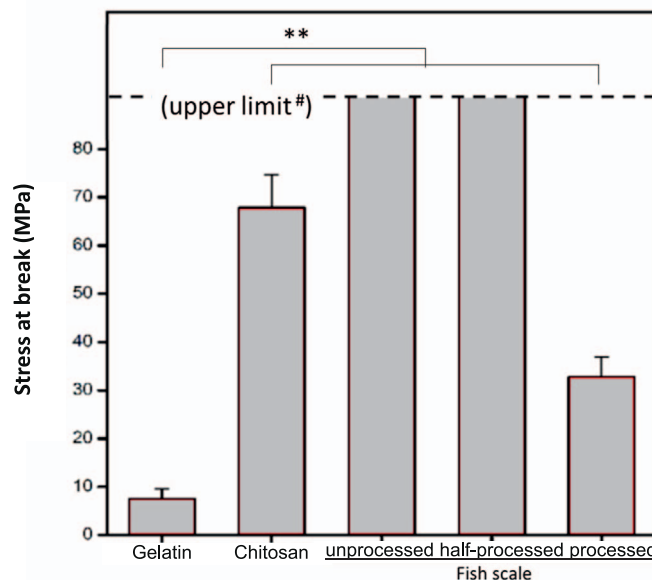


Figure 1. Physical property tests of different carrier materials. Optical transmission curves for the visible spectrum (A) and tensile strength at the breaking point (B) of different carrier materials (including gelatin, chitosan, unprocessed fish scales, half-processed fish scales, and processed fish scales) were examined. The optical transmission value of fish scales increased after processing and was higher than that of chitosan and lower than that of gelatin. The mechanical strength of fish scales decreased after processing and was higher than that of gelatin and lower than that of chitosan ($n = 3$; $**P < 0.01$). (Upper limit#): The material did not break at the loading measurement limit of the instrument.

The results showed that no significant differences in expression levels at either the RNA or protein levels were observed between attached and unattached B4G12 cells (Figs. 4A, 4B). Immunofluorescence revealed the expression patterns of ZO-1 and ATPase, suggesting that tight junctions and pump protein were maintained in the ECM protein-coated groups (Fig. 4C).

Cell adhesion was also examined using cell counting. Compared with the noncoated (C) groups, ECM protein coating significantly increased the number of cells that adhered to the fish scales (C $100\% \pm 11.1\%$, FN 215.1%

$\pm 10.2\%$, LN $230.6\% \pm 16.7\%$, Col IV $186.3\% \pm 6.7\%$, FNC $239.5\% \pm 6.7\%$). Furthermore, the cell-adhesion effect of the FNC coating was significantly better than those for the FN or Col IV coatings (Fig. 4D).

Effects of ECM Protein Coating on Cell Proliferation

We then performed cell counting and BrdU labeling to examine the effect of ECM protein coating on cell proliferation. Cell numbers were counted from

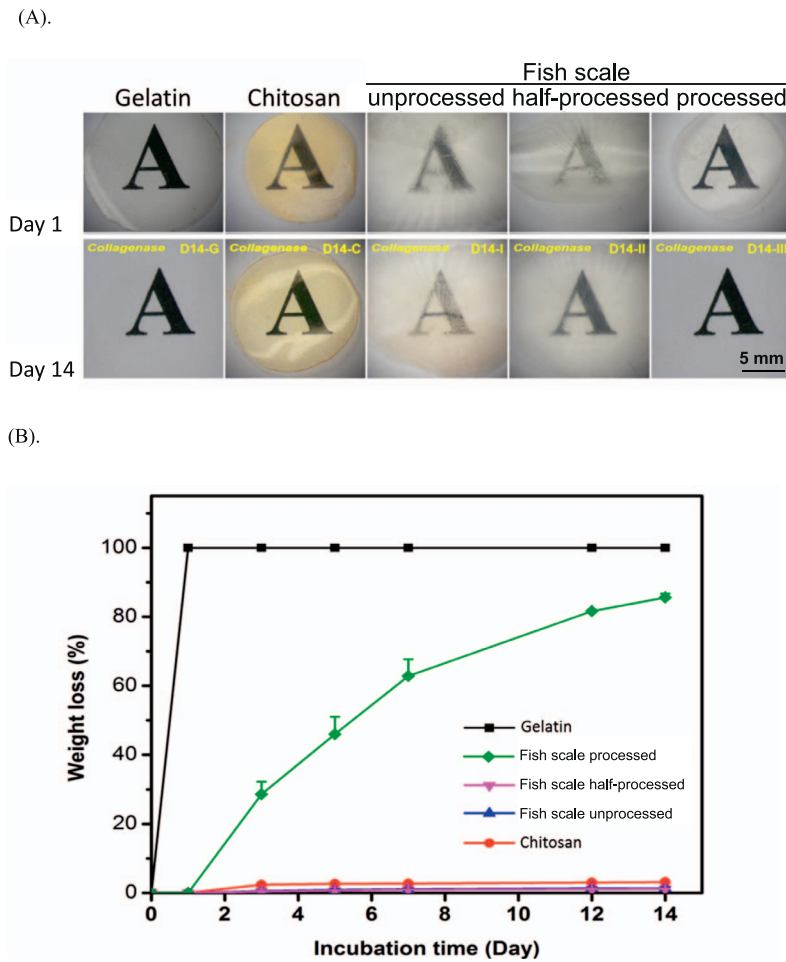


Figure 2. Biodegradability studies for different carrier materials. All carrier material samples were immersed in 12 $\mu\text{g/mL}$ collagenase solution. Gross appearance (A) and weight loss (B) were observed before and after 14 days of degradation. The weight of the processed fish scales decreased in the collagenase solution over time. (The scale bar represents 5 mm, $n = 3$).

days 1 to 4. The cell counts were significantly higher in the LN, Col IV, and FNC groups than in the noncoated (C) and FN groups (C $120.3\% \pm 2.9\%$, FN $112.9\% \pm 4.2\%$, LN $148.8\% \pm 13.6\%$, Col IV $145.5\% \pm 4.3\%$, FNC $140.2\% \pm 4.8\%$) (Fig. 5A). BrdU-positive cells were also detected 2.5 hours after BrdU labeling (Fig. 5B) in all groups, except for the noncoated group, in which BrdU labeling and detection were not possible due to the formation of cell aggregates (FN $26.1\% \pm 3.9\%$, LN $41.3\% \pm 8.4\%$, Col IV $45.2\% \pm 8.4\%$, FNC $45.7\% \pm 7.5\%$), indicating that ECM protein coating (except fibronectin) promoted cell proliferation.

Effects of ECM Surface Coating on ILK Signaling and Growth Regulation

As ECM protein coating provides ligands for integrin binding, we speculated that the integrin

signaling pathway was likely to be affected by protein coating. We previously observed that surface changes for a carrier may affect cell proliferation through the ILK/ β -catenin/p63 signaling cascade.³⁶ Integrins have been reported to be involved in the regulation of HCEC proliferation.³⁷ We previously observed that PI3K/Akt signaling was involved in cyclin D1 and p27^{Kip1} expression and in cell proliferation in B4G12 cells.³⁸ Therefore, we further examined changes in the ILK/ β -catenin/p63 pathway and the expression of cell cycle-regulating proteins (cyclin D1 and p27^{Kip1}) immunoblotting.

We observed that B4G12 cells expanded and proliferated on noncoated plastic dishes. The phosphorylation levels of ILK-T173 (p-ILK), and the protein expression levels of p63, cyclin D1 and p27^{Kip1} were not significantly different between cells cultured on noncoated dishes and those cultured on

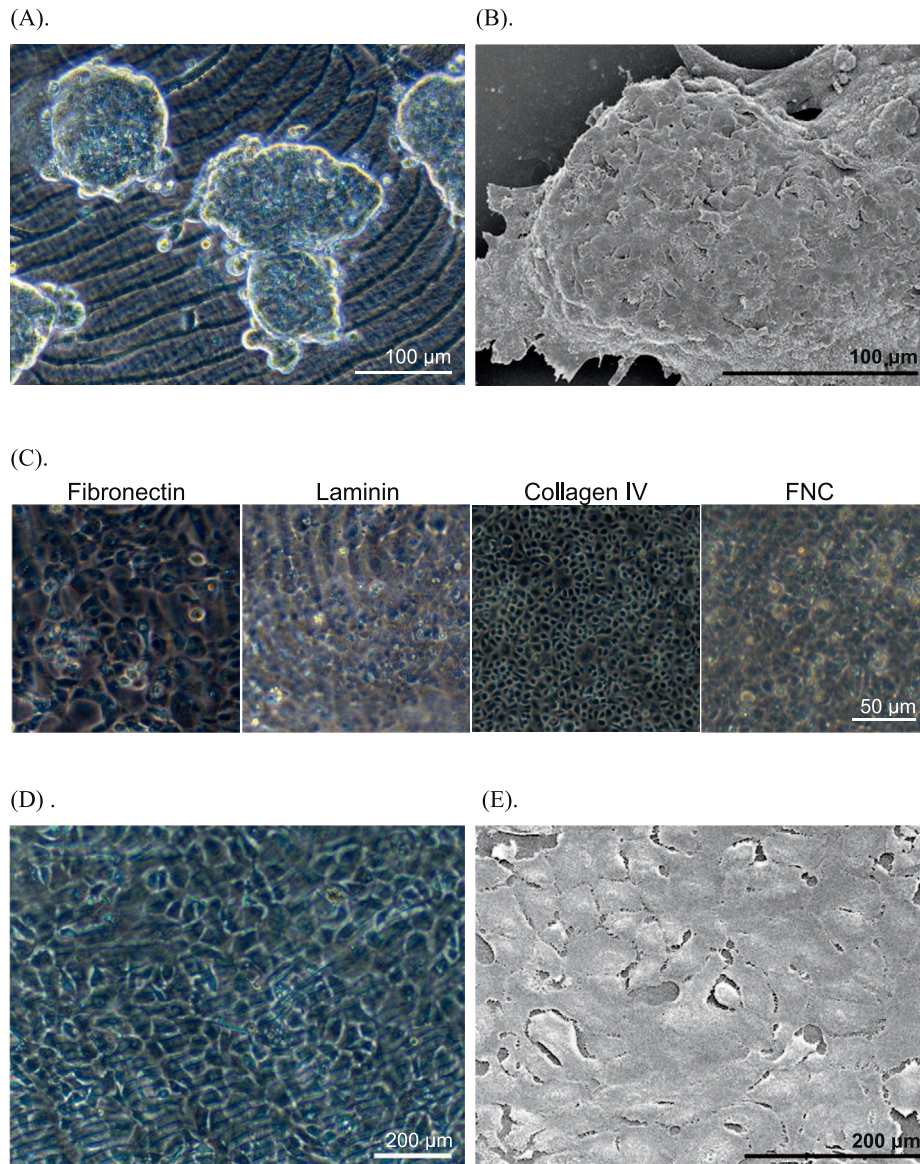


Figure 3. Cytopatibility tests on fish scale surfaces. The immortalized HCECs (B4G12 cells) were subcultured on the surfaces of non-ECM-protein-coated fish scales, and cell attachment was examined 48 hours later, using phase contrast microscopy (A) and SEM (B). Improvements to cytopatibility by ECM protein coating were observed using phase contrast microscopy (C). The primary HCECs were also subcultured on FNC-coated fish scales, and cell attachment was examined 3 weeks later, using phase contrast microscopy (D) and SEM (E). The scale bar represents 100 μm (A, B), 50 μm (C), and 200 μm (D, E).

FNC-coated plastic dishes. However, when cells were cultured on noncoated fish scales, the cells failed to expand and instead agglomerated, and the p-ILK, p63, and cyclin D1 levels decreased, while the p27^{Kip1} levels increased (Supplementary Fig. S1).

As seen in Figure 6, the results showed that, when cells were cultured on noncoated fish scales, p-ILK and p63 were highly expressed in the LN, Col IV, and FNC groups compared with the FN and control groups. However, no significant difference in the

nuclear translocation of β -catenin was found. In addition, increased cyclin D1 expression and decreased p27^{Kip1} expression were observed in the FNC groups.

Discussion

Cell transplant carriers play an indispensable role in tissue engineering. In addition to facilitating surgery, cell carriers provide a microenvironment for

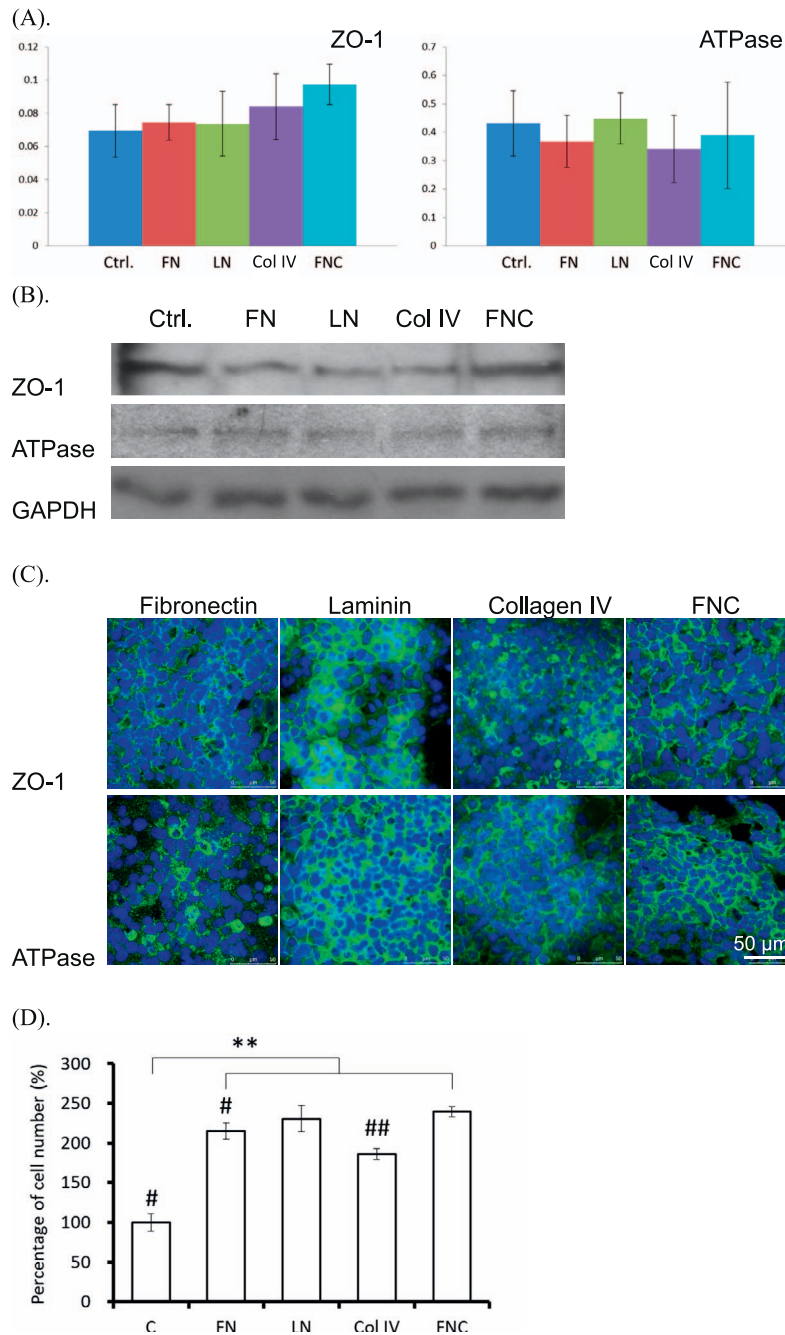


Figure 4. Cell adhesion tests on ECM protein-coated fish scales. B4G12 cells were subcultured on ECM-protein-coated fish scales. q-PCR (A), immunoblotting (B), and immunofluorescence (C) were used to examine the expression and location of HCEC markers (ZO-1 and ATPase). Nuclei were counterstained with Hoechst 33342 (blue). The scale bar represents 50 μm . (D) The effect of ECM proteins on cell adhesion was examined using cell counting. Compared with the noncoated groups, ECM protein coating significantly increased the numbers of adherent cells. The cell-adhesive effect of FNC coating was significantly better than those of FN or Col IV coating (** $P < 0.01$ versus control group, # $P < 0.05$, ## $P < 0.01$ versus FNC group, $n = 3$).

cell growth and regulate physiological and biochemical reactions in cells. Thus, relevant research and applications are key aspects of tissue engineering. According to previously published reports, the mean optical transmission of processed fish scales was

90%,²⁴ whereas the optical transmission of the human cornea was 91%.⁴⁵ In the present study, we confirmed that processed fish scales had a high optical transmittance, better than that of chitosan materials and close to that of gelatin (Fig. 1A). As seen in Figure

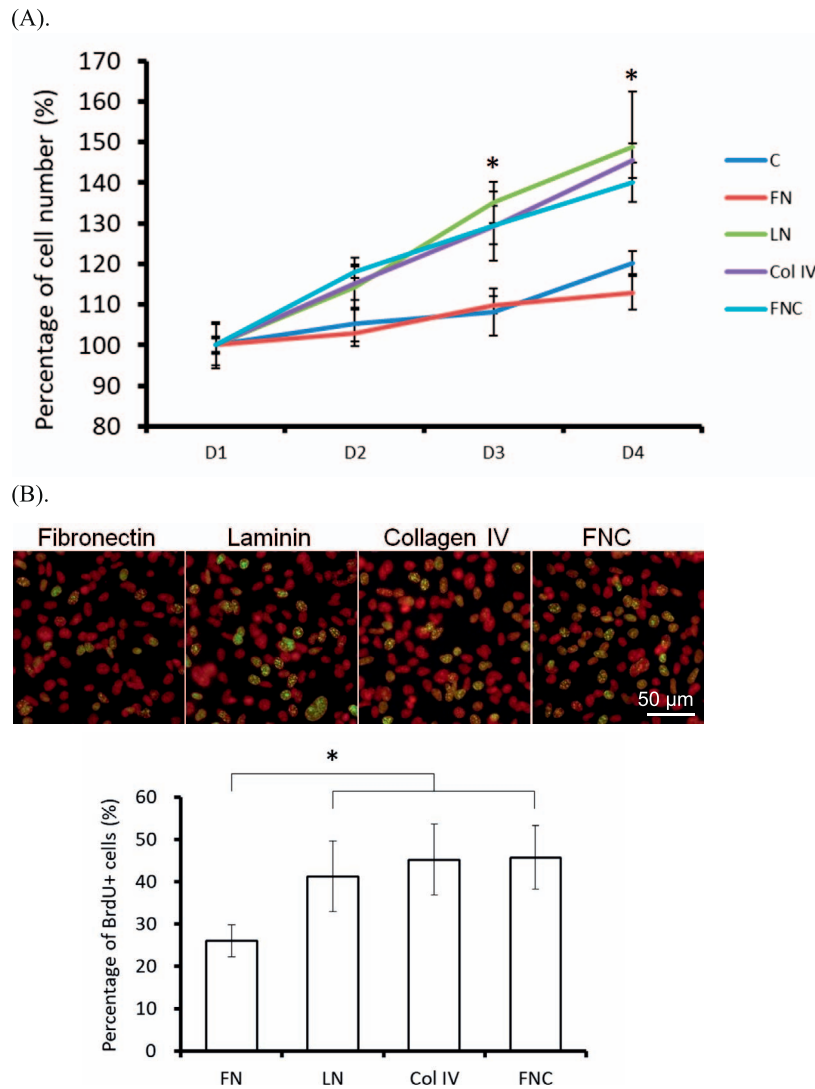


Figure 5. Effects of ECM protein coating on cell proliferation. Cell proliferation was examined using cell counting (A) and BrdU labeling (B). (A) ECM protein coating (except fibronectin) significantly increased the cell counts ($n = 3$; $*P < 0.05$ LN, Col IV, and FNC group versus control group). (B) The percentages of BrdU-positive cells (green, nuclei were counterstained with propidium iodide; the scale bar represents 50 μm) in the LN-, Col IV-, and FNC-coated groups were significantly higher than that in the fibronectin-coated group ($n = 3$; $*P < 0.05$).

IB, the results showed that, although gelatin has a high level of transmittance, its poor material strength made it difficult to manage in surgery and prone to damage during the transplantation and suture processes. In contrast, the physical properties of processed fish scales were suitable for surgical operations. In addition, Van Essen et al.²⁴ implanted fish scales into rat corneas for biocompatibility testing and did not observe significant changes in the fish scale structure after 3 weeks. Because the fish scale is composed of collagen I and its weight decreased in collagenase solution over time, it is possible that fish scales fuse with the host tissue through tissue

remodeling after long-term implantation. The round-shaped size and curvature of processed fish scales may be obtained by stamping. Moreover, after ECM protein coating, processed fish scales also have good cytocompatibility. Therefore, we believe that fish scales have potential as cell carriers for transplantation surgery.

Although B4G12 cells are immortalized HCECs that retain normal morphology, they have several different properties compared with primary cells. First, the in vitro proliferation capacity of primary HCECs is limited by contact inhibition, and monolayers are formed upon reaching confluence, which

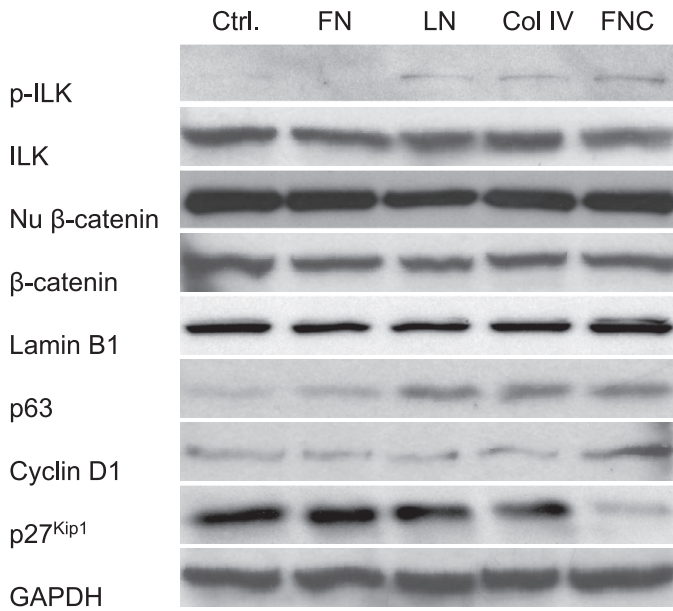


Figure 6. Effects of the ECM protein coating on ILK signaling and cell proliferation regulators. Protein expression levels of ILK-related signaling molecules and cell proliferation regulators were analyzed with immunoblotting. The fish scales were coated with various types of ECM proteins and then seeded with B4G12 cells. After 48 hours, nuclear extracts (Nu) or total lysates were collected and subjected to immunoblotting using a series of antibodies. Lamin B1 and GAPDH were used as loading controls. p-ILK and p63 were highly expressed in the LN, Col IV, and FNC groups compared with the FN and control groups. Increased cyclin D1 expression and decreased p27^{Kip1} expression were observed in the FNC group.

may persist for 2 months on FNC-coated plastic dishes. In this study, we observed the maintenance of normal morphology and monolayer formation in HCECs that were seeded on FNC-coated fish scales up to day 21 (Figs. 3D, 3E). In contrast, proliferation persisted in confluent B4G12 cells, as stratified cell layers formed, which may hamper their clinical applicability. Second, regular commercial plastic dishes are often treated for optimum attachment and growth⁴⁶ (e.g., tissue culture treated by the Corning, Inc.). B4G12 cells have stronger adhesive abilities and can expand, proliferate, and subculture on noncoated plastic dishes, while primary HCECs require ECM-coating (e.g., collagen IV or FNC) to improve cell expansion. Despite their stronger adhesive properties, B4G12 cells failed to expand and instead agglomerated on noncoated fish scales but could expand on FNC-coated fish scales after ECM coating. Due to fundamental differences between the use of a cell line and primary cells, we also examined the biocompatibility of FNC-coated fish scales using primary HCECs (Figs. 3D, 3E). Interestingly, Parekh

et al.²⁷ also reported the proliferation of HCECs on FNC-coated fish scales.

In corneal tissue, HCECs adhere to Descemet's membrane (DM). DM consists of a variety of ECM proteins, including collagens (Col IV and Col VIII), LNs (332, 411, and 511),⁴⁷ and FN.^{48,49} Examining the effects of ECM protein coating on HCECs, Choi et al.⁵⁰ reported that Col I, Col IV, FN, and FNC significantly increased HCEC adhesion and proliferation. In the present study, we observed that ECM proteins effectively promoted the adhesion and proliferation of B4G12 cells on fish scales. We found that different types of ECM coatings had different effects on ILK activation and the expression of p63 and cell cycle mediators (cyclin D1 and p27^{Kip1}). An increase in cell proliferation and p-ILK and p63 expression levels were observed in the LN, Col IV, and FNC groups, which indicated that, except for FN, ECM coatings may affect integrin pathway activation and cell proliferation. Because p63 effects the cell cycle by modulating p53 target genes,⁵¹ LN, Col IV, and FNC might affect cell proliferation through p63-dependent pathways. However, p63 was upregulated in the LN, Col IV, and FNC groups, while increased levels of cyclin D1 and decreased levels of p27^{Kip1} were only found in the FNC group, indicating that FNC affects cyclin D1 and p27^{Kip1} via p63-independent pathways. Nevertheless, this hypothesis requires further validation.

Conclusions

This study focused on tissue engineering development and aimed to explore new functions for biomaterials that have been proven to be safe. Based on the results of this study, we believe that processed fish scales merit verification as an HCEC carrier. Once their function is tested in animal models, this material may be applied as a clinical cell therapy (e.g., c-DSAEK).

Acknowledgments

The authors thank the Microscopy Core Laboratory at Chang Gung Memorial Hospital, Linkou, for providing technical assistance.

Supported by grants from the Ministry of Science and Technology, Taiwan (grant number 107-2314-B-182A-122; to DHKM), and Chang Gung Memorial Hospital (grant numbers CMRPG3G0021-3,

CMRPG3F1471-2, and CMRPG3G0031-3; to DHKM and HCC).

Disclosure: **Y.-J. Hsueh**, None; **D.H.-K. Ma**, None; **K.S.-C. Ma**, None; **T.-K. Wang**, None; **C.-H. Chou**, Body Organ Biomedical Corporation (E); **C.-C. Lin**, Body Organ Biomedical Corporation (E); **M.-C. Huang**, Body Organ Biomedical Corporation (E); **L.-J. Luo**, None; **J.-Y. Lai**, None; **H.-C. Chen**, None

*Yi-Jen Hsueh and David Hui-Kang Ma contributed equally to this article.

References

- Iwamoto T, Smelser GK. Electron microscopy of the human corneal endothelium with reference to transport mechanisms. *Invest Ophthalmol*. 1965;4:270–284.
- Kreutziger GO. Lateral membrane morphology and gap junction structure in rabbit corneal endothelium. *Exp Eye Res*. 1976;23:285–293.
- Maurice DM. The location of the fluid pump in the cornea. *J Physiol*. 1972;221:43–54.
- Geroski DH, Edelhauser HF. Quantitation of Na/K ATPase pump sites in the rabbit corneal endothelium. *Invest Ophthalmol Vis Sci*. 1984;25:1056–1060.
- Fischbarg J, Lim JJ. Role of cations, anions and carbonic anhydrase in fluid transport across rabbit corneal endothelium. *J Physiol*. 1974;241:647–675.
- Sherrard ES. The corneal endothelium in vivo: its response to mild trauma. *Exp Eye Res*. 1976;22:347–357.
- Kaufman HE, Katz JI. Pathology of the corneal endothelium. *Invest Ophthalmol Vis Sci*. 1977;16:265–268.
- Joyce NC, Mekler B, Neufeld AH. In vitro pharmacologic separation of corneal endothelial migration and spreading responses. *Invest Ophthalmol Vis Sci*. 1990;31:1816–1826.
- Ku BI, Hsieh YT, Hu FR, Wan IJ, Chen WL, Hou YC. Endothelial cell loss in penetrating keratoplasty, endothelial keratoplasty, and deep anterior lamellar keratoplasty. *Taiwan J Ophthalmol*. 2017;7:199–204.
- Gorovoy MS. Descemet-stripping automated endothelial keratoplasty. *Cornea*. 2006;25:886–889.
- Honda N, Mimura T, Usui T, Amano S. Descemet stripping automated endothelial keratoplasty using cultured corneal endothelial cells in a rabbit model. *Arch Ophthalmol*. 2009;127:1321–1326.
- Doillon CJ, Watsky MA, Hakim M, et al. A collagen-based scaffold for a tissue engineered human cornea: physical and physiological properties. *Int J Artif Organs*. 2003;26:764–773.
- Lu PL, Lai JY, Ma DH, Hsiue GH. Carbodiimide cross-linked hyaluronic acid hydrogels as cell sheet delivery vehicles: characterization and interaction with corneal endothelial cells. *J Biomater Sci Polym Ed*. 2008;19:1–18.
- Rafat M, Li F, Fagerholm P, et al. PEG-stabilized carbodiimide crosslinked collagen-chitosan hydrogels for corneal tissue engineering. *Biomaterials*. 2008;29:3960–3972.
- Wang TJ, Wang IJ, Chen S, Chen YH, Young TH. The phenotypic response of bovine corneal endothelial cells on chitosan/polycaprolactone blends. *Colloids Surf B Biointerfaces*. 2012;90:236–243.
- Niu G, Choi JS, Wang Z, Skardal A, Giegengack M, Soker S. Heparin-modified gelatin scaffolds for human corneal endothelial cell transplantation. *Biomaterials*. 2014;35:4005–4014.
- Bayyoud T, Thaler S, Hofmann J, et al. Decellularized bovine corneal posterior lamellae as carrier matrix for cultivated human corneal endothelial cells. *Curr Eye Res*. 2012;37:179–186.
- Sugiura H, Yunoki S, Kondo E, Ikoma T, Tanaka J, Yasuda K. In vivo biological responses and bioresorption of tilapia scale collagen as a potential biomaterial. *J Biomater Sci Polym Ed*. 2009;20:1353–1368.
- Chen S, Hirota N, Okuda M, et al. Microstructures and rheological properties of tilapia fish-scale collagen hydrogels with aligned fibrils fabricated under magnetic fields. *Acta Biomater*. 2011;7:644–652.
- Ikoma T, Kobayashi H, Tanaka J, Walsh D, Mann S. Microstructure, mechanical, and biomimetic properties of fish scales from *Pagrus major*. *J Struct Biol*. 2003;142:327–333.
- Yuan F, Wang L, Lin CC, Chou CH, Li L. A cornea substitute derived from fish scale: 6-month follow up on rabbit model. *J Ophthalmol*. 2014;2014:914542.
- Okuda M, Takeguchi M, Tagaya M, et al. Elemental distribution analysis of type I collagen fibrils in tilapia fish scale with energy-filtered transmission electron microscope. *Micron*. 2009;40:665–668.
- Chou CH, Chen YG, Lin CC, Lin SM, Yang KC, Chang SH. Bioabsorbable fish scale for the

- internal fixation of fracture: a preliminary study. *Tissue Eng Part A*. 2014;20:2493–2502.
24. van Essen TH, Lin CC, Hussain AK, et al. A fish scale-derived collagen matrix as artificial cornea in rats: properties and potential. *Invest Ophthalmol Vis Sci*. 2013;54:3224–3233.
 25. van Essen TH, van Zijl L, Possemiers T, et al. Biocompatibility of a fish scale-derived artificial cornea: cytotoxicity, cellular adhesion and phenotype, and in vivo immunogenicity. *Biomaterials*. 2016;81:36–45.
 26. Chen SC, Telinius N, Lin HT, et al. Use of fish scale-derived biocornea to seal full-thickness corneal perforations in pig models. *PLoS One*. 2015;10:e0143511.
 27. Parekh M, Van den Bogerd B, Zakaria N, Ponzin D, Ferrari S. Fish scale-derived scaffolds for culturing human corneal endothelial cells. *Stem Cells Int*. 2018;2018:11.
 28. Symington BE. Fibronectin receptor modulates cyclin-dependent kinase activity. *J Biol Chem*. 1992;267:25744–25747.
 29. Mortarini R, Gismondi A, Santoni A, Parmiani G, Anichini A. Role of the alpha 5 beta 1 integrin receptor in the proliferative response of quiescent human melanoma cells to fibronectin. *Cancer Res*. 1992;52:4499–4506.
 30. Park JH, Ryu JM, Han HJ. Involvement of caveolin-1 in fibronectin-induced mouse embryonic stem cell proliferation: role of FAK, RhoA, PI3K/Akt, and ERK 1/2 pathways. *J Cell Physiol*. 2011;226:267–275.
 31. Cordes N, van Beuningen D. Cell adhesion to the extracellular matrix protein fibronectin modulates radiation-dependent G2 phase arrest involving integrin-linked kinase (ILK) and glycogen synthase kinase-3beta (GSK-3beta) in vitro. *Br J Cancer*. 2003;88:1470–1479.
 32. Chen HM, Lin YH, Cheng YM, Wing LY, Tsai SJ. Overexpression of integrin-beta1 in leiomyoma promotes cell spreading and proliferation. *J Clin Endocrinol Metab*. 2013;98:E837–E846.
 33. Schiller HB, Hermann MR, Polleux J, et al. Beta1- and alpha-v-class integrins cooperate to regulate myosin II during rigidity sensing of fibronectin-based microenvironments. *Nature Cell Biol*. 2013;15:625–636.
 34. Chen J, Guerriero E, Lathrop K, SundarRaj N. Rho/ROCK signaling in regulation of corneal epithelial cell cycle progression. *Invest Ophthalmol Vis Sci*. 2008;49:175–183.
 35. Hsueh YJ, Chen HC, Chu WK, et al. STAT3 regulates the proliferation and differentiation of rabbit limbal epithelial cells via a DeltaNp63-dependent mechanism. *Invest Ophthalmol Vis Sci*. 2011;52:4685–4693.
 36. Ma DH, Chen HC, Ma KS, et al. Preservation of human limbal epithelial progenitor cells on carbodiimide cross-linked amniotic membrane via integrin-linked kinase-mediated Wnt activation. *Acta Biomater*. 2016;31:144–155.
 37. Yamaguchi M, Ebihara N, Shima N, et al. Adhesion, migration, and proliferation of cultured human corneal endothelial cells by laminin-5. *Invest Ophthalmol Vis Sci*. 2011;52:679–684.
 38. Hsueh YJ, Chen HC, Wu SE, Wang TK, Chen JK, Ma DH. Lysophosphatidic acid induces YAP-promoted proliferation of human corneal endothelial cells via PI3K and ROCK pathways. *Mol Ther Methods Clin Dev*. 2015;2:15014.
 39. Lin CC, Ritch R, Lin SM, et al. A new fish scale-derived scaffold for corneal regeneration. *Eur Cells Materials*. 2010;19:50–57.
 40. Lai JY, Li YT, Cho CH, Yu TC. Nanoscale modification of porous gelatin scaffolds with chondroitin sulfate for corneal stromal tissue engineering. *Int J Nanomedicine*. 2012;7:1101–1114.
 41. Lai J-Y, Wang T-P, Li Y-T, Tu IH. Synthesis, characterization and ocular biocompatibility of potential keratoprosthesis hydrogels based on photopolymerized poly(2-hydroxyethyl methacrylate)-co-poly(acrylic acid). *J Materials Chem*. 2012;22:1812–1823.
 42. Ma DH, Lai JY, Cheng HY, Tsai CC, Yeh LK. Carbodiimide cross-linked amniotic membranes for cultivation of limbal epithelial cells. *Biomaterials*. 2010;31:6647–6658.
 43. Li W, Sabater AL, Chen YT, et al. A novel method of isolation, preservation, and expansion of human corneal endothelial cells. *Invest Ophthalmol Vis Sci*. 2007;48:614–620.
 44. Valtink M, Gruschwitz R, Funk RH, Engelmann K. Two clonal cell lines of immortalized human corneal endothelial cells show either differentiated or precursor cell characteristics. *Cells Tissues Organs*. 2008;187:286–294.
 45. van den Berg TJ, Tan KE. Light transmittance of the human cornea from 320 to 700 nm for different ages. *Vis Res*. 1994;34:1453–1456.
 46. Ramsey WS, Hertl W, Nowlan ED, Binkowski NJ. Surface treatments and cell attachment. *In Vitro*. 1984;20:802–808.
 47. Kabosova A, Azar DT, Bannikov GA, et al. Compositional differences between infant and

- adult human corneal basement membranes. *Invest Ophthalmol Vis Sci.* 2007;48:4989–4999.
48. Suda T, Nishida T, Ohashi Y, Nakagawa S, Manabe R. Fibronectin appears at the site of corneal stromal wound in rabbits. *Curr Eye Res.* 1981;1:553–556.
 49. Fujikawa LS, Foster CS, Harrist TJ, Lanigan JM, Colvin RB. Fibronectin in healing rabbit corneal wounds. *Lab Invest.* 1981;45:120–129.
 50. Choi JS, Kim EY, Kim MJ, et al. In vitro evaluation of the interactions between human corneal endothelial cells and extracellular matrix proteins. *Biomed Mater.* 2013;8:014108.
 51. Dohn M, Zhang S, Chen X. p63alpha and DeltaNp63alpha can induce cell cycle arrest and apoptosis and differentially regulate p53 target genes. *Oncogene.* 2001;20:3193–3205.